Eugeniusz KURGAN, Piotr GAS

AGH University of Science and Technology

Treatment of Tumors Located in the Human Thigh using RF Hyperthermia

Abstract. *In this publication a numerical model and simulation results of electric field, induced current density and temperature distributions inside human thigh heated by external RF hyperthermia are presented. For simplicity, the heat transfer problem is treated in two-dimensions with semi-infinite tissue model. The bioheat equation under a transient-time condition is solved to determine the temperature distributions inside the tumor and surrounding tissues. The heat removal due to the blood circulation is also taken into account in the presented model.*

Streszczenie. *W niniejszym artykule przedstawiono model numeryczny i wyniki symulacji pola elektrycznego, gęstości prądu indukowanego i rozkładów temperatury wewnątrz ludzkiego uda grzanego przy użyciu zewnętrznej RF hipertermii. Dla uproszczenia problem wymiany ciepła jest rozpatrywany w dwóch wymiarach dla pół-nieskończonego modelu tkanek. W celu określenia rozkładu temperatury wewnątrz guza i w otaczających go tkankach rozwiązano biologiczne równanie ciepła w przypadku zmiennym w czasie. W rozważanym modelu uwzględniono również odprowadzanie ciepła wynikające z krążenia krwi.* ***(Leczenie guzów zlokalizowanych w udzie człowieka przy użyciu RF hipertermii)***

Keywords: hyperthermia, bioheat equation, temperature distribution, finite element method
Słowa kluczowe: hipertermia, biologiczne równanie ciepła, rozkład temperatury, metoda elementów skończonych

Introduction

Successful applications of the electromagnetic stimulation with the aid of low frequency fields for the treatment of tumors, heavy wounds and some neural diseases have been widely reported [2]. There is evidence that hyperthermia can significantly reduce the time needed for health recovery, but it is not clear how it works and how it should be effectively applied [1]. Radiofrequency hyperthermia with exiting electromagnetic field at frequencies of about 100 MHz [4], based on destructive properties of heat on the tumor, can be helpful as an additional tool in the traditional radiotherapy and chemotherapy treatment of malignant tumors situated not to deep under the skin in the human body [12]. Some clinical studies have demonstrated the efficiency of thermal therapy in suspending tumor growth [11]. Numerical modelling of optimal temperature distribution in radiofrequency hyperthermia can be helpful in identifying better treatments.

Hyperthermia treatment involves heating the tumor tissue to temperature greater than 42°C without exceeding the normal physiologic temperature range in healthy tissues, which is lower than 42°C. The working temperature range is thus very small. If the tumor temperature is lower as 42°C, there is no therapeutic effect. If the temperature is greater than 44 – 45°C both normal and tumor cells are damaged [3]. Because blood vessels in tumor tissues have greater diameters then in normal tissues, and thus occupy greater volume, tumor temperature is usually greater than that of the surrounding tissue during hyperthermia therapy. This is caused by the fact that blood has usually greater conductivity than cancerous cells. In addition, one believes that tumor tissues are more sensitive to heat. Hypoxic and cancerous cells are resistive to radiation, and hyperthermia can help by thermally killing them. Heating tissue methods involve whole body heating using hot wax, hot air, hot water bath, infrared, or partial body heating utilizing radiofrequency (RF), microwave, ultrasound, hot blood, or fluid perfusion. Only the last three methods allows for deep tissue heating. Generally, it is not easy to obtain an accurate determination of the temperature field over the entire treatment region during clinical hyperthermia treatments, because the number of invasive temperature probes that can be used is limited due to the pain tolerance of patients. Furthermore, to ensure that the temperature is within the desired range, the clinician usually monitors the temperature every few seconds by pressing the hold button of the thermocouple needle, and at the same time keeps the thermocouple needle away from the light spot. Thus, it is desirable to develop a mathematical method that can determine the power intensity and the pattern of laser or radiation exposure in order to optimize the temperature distribution in the target region before treatment. In this manner, the treatment efficiency can be assessed more precisely [9]. There are many studies on the treatment of cancer using hyperthermia which demonstrates that this aspect is still important and more research is needed in this matter [6, 8].

In this article electric field and temperature distribution inside cross a section across of a human thigh with a bone and the tumor inside are calculated.

Main equations

Let us consider a cross section of the human thigh as it is depicted in Fig.1.

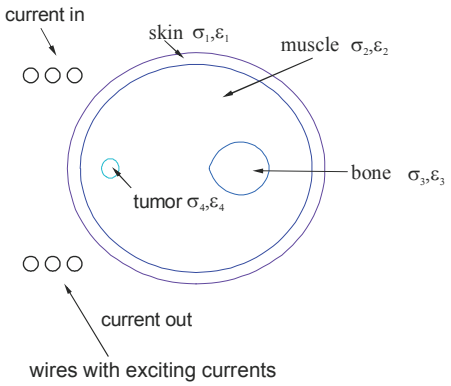

Fig.1. Simplified version of transverse section across human thigh with the tumor inside

It is assumed that human thigh and the bone inside have an ellipsoidal shape and the tumor has a circular form with radius R. Skin thickness is equal to d. Near the human thigh a coil made of several wires with exciting currents is placed. The radius of each wire is equal to r. The exciting current in wires generates sinusoidal electromagnetic field which next induces eddy currents in the human body. These currents are sources of heat and after some transient time a temperature distribution in the body is established [12].

Let us start with Maxwell's equations in the frequency domain:

(1) $$\nabla \times \mathbf{H} = \mathbf{J}_i + \mathbf{J}_c + j\omega \mathbf{D}$$

(2) $$\nabla \times \mathbf{E} = -j\omega \mathbf{B}$$

where $\mathbf{E}$ and $\mathbf{H}$ are respectively the electric and magnetic field strengths, $\mathbf{J}_i$ is an impressed current density, which is treated as a source of electromagnetic field, $\mathbf{J}_c$ is conduction current resulting from the existence of an electric field according to Ohm's law

(3) $$\mathbf{J}_c = \sigma \mathbf{E}$$

where σ is the electrical conductivity of the body. $\mathbf{D}$ and $\mathbf{B}$ are respectively the vectors of electric displacement density and magnetic induction given in the form of material dependences

(4) $$\mathbf{D} = \varepsilon \mathbf{E} \quad , \quad \mathbf{B} = \mu \mathbf{H}$$

where ε and μ are respectively the permittivity and magnetic permeability of the medium. After the introduction of the magnetic vector potential $\mathbf{B} = \nabla \times \mathbf{A}$ we can derive the following equation describing the field distribution:

(5) $$\nabla \times \left(\frac{1}{\mu} \nabla \times \mathbf{A} \right) + \omega \left(j\sigma - \omega\varepsilon \right) \mathbf{A} = \mathbf{J}_i$$

Since the magnetic vector potential (as well as other vectors) in the time domain is related with complex amplitude by

(6) $$\mathbf{A}(\mathbf{r}, t) = \mathrm{Re}\left[\hat{\mathbf{A}}(\mathbf{r}) e^{j\omega t} \right]$$

therefore equation (7) in the complex domain is given by

(7) $$\nabla \times \left(\frac{1}{\mu} \nabla \times \hat{\mathbf{A}} \right) + \omega \left(j\sigma - \omega\hat{\varepsilon} \right) \hat{\mathbf{A}} = \hat{\mathbf{J}}_i$$

where $\hat{\varepsilon}$ is the complex permittivity defined as

(8) $$\hat{\varepsilon}(\omega) = \varepsilon' - j\varepsilon''$$

where ε' is the real part of the permittivity, which is related to the stored energy within the medium and ε'' is a dielectric loss factor (it is the imaginary part of the permittivity, which is related to the dissipation (or loss) of energy within the medium).
For one Debye's process [5] we can assume that

(9) $$\hat{\varepsilon}(\omega) = \varepsilon_\infty + \frac{\Delta\varepsilon_1}{1 + \left(j\omega\tau_1 \right)^{\alpha_1}} - j\frac{\sigma_1}{\omega\varepsilon_0}$$

where ε_∞ is the high-frequency limit of relative permittivity, $\Delta\varepsilon_1$ is the relaxation intensity, α_1 the Cole–Cole parameter and τ_1 the relaxation time.
Magnetic vector potential and exciting current density are perpendicular to the plane x-y and their modules are complex numbers and have real and imaginary parts:

(10) $$\hat{\mathbf{A}} = \hat{A}_z \mathbf{e}_z = (A_{zr} + jA_{zi}) \mathbf{e}_z$$

(11) $$\hat{\mathbf{J}} = \hat{J}_z \mathbf{e}_z = (J_{zr} + jJ_{zi}) \mathbf{e}_z$$

After substituting equations (7) and (8) into equation (6) and comparison of real and imaginary parts we obtain:

(12) $$\nabla \times \left(\frac{1}{\mu} \nabla \times A_{zr} \right) - \omega \left(\omega\hat{\varepsilon} A_{zr} + \sigma A_{zi} \right) = J_{zr}$$

(13) $$\nabla \times \left(\frac{1}{\mu} \nabla \times A_{zi} \right) + \omega \left(\sigma A_{zr} - \omega\hat{\varepsilon} A_{zi} \right) = J_{zi}$$

The total electric field is related to the vector potential by

(14) $$\hat{\mathbf{E}} = -j\omega\hat{\mathbf{A}} = \omega(A_{zi} - jA_{zr}) \mathbf{e}_z$$

Eddy currents induced in the human body are calculated from

(15) $$\hat{\mathbf{J}} = \sigma\hat{\mathbf{E}} = \omega\sigma(A_{zi} - jA_{zr}) \mathbf{e}_z$$

The mean electric power released in the conducting body is given by

(16) $$p = \sigma\hat{\mathbf{E}} \cdot \hat{\mathbf{E}}^* = \sigma \left| \hat{\mathbf{E}} \right|^2 = \sigma\omega^2 \left(A_{zr}^2 + A_{zi}^2 \right)$$

Unlike the computation of electric currents in body, for which agreement exists as to the derived physical model, no clear consensus exists for an appropriate mathematical model for the evaluation of temperature field distribution in biological tissues. An extremely important work in the modelling of heat transfer in biological tissues was done over half a century ago by Pennes [10]. The equation, which he derived, is named bioheat equation, and it can be derived from the classical Fourier law of heat conduction. Pennes model is based on the simple assumption of the energy exchange between the blood flowing in vessels and the surrounding the tumor tissues. It may provide suitable information on temperature distributions in the whole body, organ under consideration, and tumor analysis under study. The Pennes model states that the total heat exchange between the tissue surrounding a vessel and the blood flowing in it, is proportional to the volumetric heat flow and the temperature difference between the blood and the tissue. The expression of Pennes bioheat equation in a body with uniform material properties in transient analysis is given by [4, 7]

(17) $$\rho C \frac{\partial T}{\partial t} + \nabla \left(-k\nabla T \right) = \rho_b C_b \omega_b (T_b - T) + Q_{ext} + Q_{met}$$

where T is the body temperature [K], k – the tissue thermal conductivity [W/(m^2 K)], ρ – the tissue density [kg/m^3], C − the tissue specific heat [J/(kg K)], T_b – the blood vessel temperature [K], ρ_b – the blood density [kg/m^3], ω_b − blood perfusion rate [1/s], C_b – the blood specific heat [J/(kg K)], Q_{met} − the metabolic heat generation rate [W/m^3]. Described model also takes into account the external heat sources Q_{ext} [W/m^3], which is responsible for the changing of the temperature inside the exposed body according to the following equation

(18) $$Q_{ext} = p = \sigma\omega^2 \left(A_{zr}^2 + A_{zi}^2 \right)$$

To the above equations both the initial and boundary conditions should be added. The usual boundary condition associated with the heat transfer process in the RF hyperthermia can be given by

(19) $$\mathbf{n} \cdot \left(-k\nabla T \right) = h(T_{air} - T)$$

where h is the heat transfer coefficient [W/(m^2·K)], T_{air} is the temperature of the air surrounding the body [K] and $\mathbf{n}$ is the unit vector normal to the surface. The initial condition is equal $T_0 = 37$ °C, which corresponds to the physiological temperature of the human body.

Equations (2), (13) and (17) with appropriate initial and boundary conditions are solved using the finite element method.

Simulation results

The main purpose of this article is the analysis of the transient temperature field in different tissues of human thigh subjected to external electromagnetic heating condition. In the analyzed model, the human body and tumor are considered as homogeneous media with averaged material parameters. For simplicity we assumed a constant value of blood perfusion rate in various biological tissues. The dimensional parameters of the model are defined in Table 1. Electrical and thermal parameters of tissues are taken from [5] and presented in Table 2. Physical parameters of blood are given in Table 3. In addition, the exciting current in all wires is given by $I_{max} = 15$ [A], and the exciting frequency is $f = 100$ [MHz]. Moreover, the heat transfer coefficient is assumed equal to $h = 5$ [W/(m^2·K)], and the temperature of the air surrounding the human body equal to $T_{air} = 293.15$ [K], which corresponds to room temperature of 20°C.

Table 1. Geometrical dimensions of the model

human body semi axes	A = 0.15 [m], B = 0.12 [m]
tumor radius	R = 0.0125 [m]
skin thickness	d = 0.0015 [m]
bone semi axes	a = 0.035 [m], b = 0.025 [m]
wire radius	r = 0.01 [m]

Table 2. Physical parameters of tissues used in the numerical model [5]

Tissue	ε_∞	$\Delta\varepsilon_1$	τ_1 [ps]	α_1	σ_1 [S/m]
muscle	4.0	50	7.23	0.10	0.15
skin	4.0	32	7.23	0.10	0.10
tumor	2.5	18	13.2	0.22	0.07
bone	4.0	40	8.84	0.10	0.70

Tissue	k [W/(m·K)]	ρ [kg/m^3]	C [J/(kg·K)]	Q_{met} [W/m^3]
muscle/skin	0.22	1050	3700	300
tumor	0.56	1050	3700	480
bone	0.013	1500	3700	120

Table 3. Physical parameters of blood taken in the bioheat equation

Tissue	ρ_b [kg/m^3]	C_b [J/(kg·K)]	T_b [K]	ω_b [1/s]	
blood	1020	3640	310.15	in tumor in muscle/skin in bone	0.005 0.0004 0.00001

The simulation results are summarized in Figures 2 – 7. Fig. 2 shows two components A_{zr} and A_{zi} together with modulus of the vector A_{zm} for the phase angel equal zero along human thigh perimeter in steady state. The imaginary part of the magnetic vector potential is substantially smaller than its real part. Analogous components of the electric field strength are shown in Fig. 3. Modulus and the real part of electric field seem to be a mirror reflection. The remaining drawings illustrate the temperature dependences in different forms. Distribution of temperature along the longer semi axis of the tight cross section for different time steps is given in Fig.4. The highest value of the temperature is in the tumor and with time exceeds 45°C. In the skin and in the bone the temperature has substantially lower and from the medical point of view it has acceptable values below 42°C. Fig. 5 represents temperature distribution along the x axis of the cross section of the tumor for different moments in time.

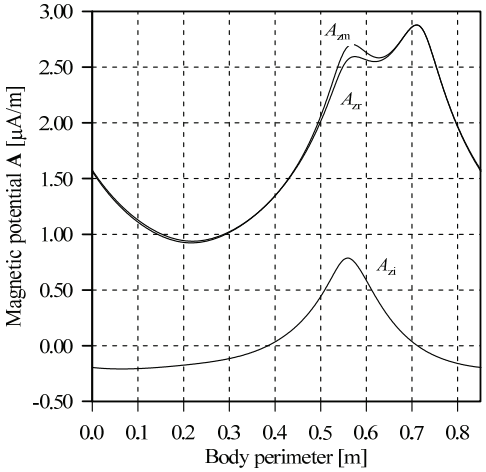

Fig.2. Components of magnetic vector potential **A** along human thigh perimeter in steady state

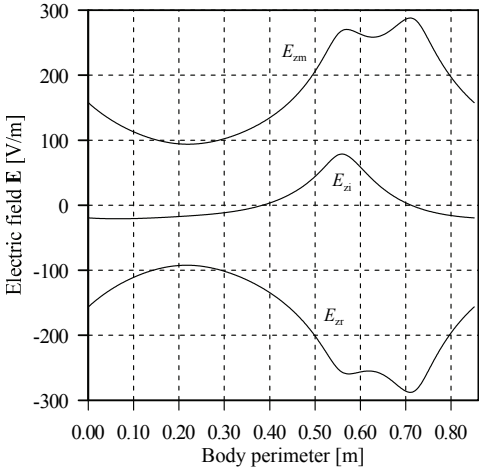

Fig.3. Components of the electric field strength **E** along human thigh perimeter in steady state

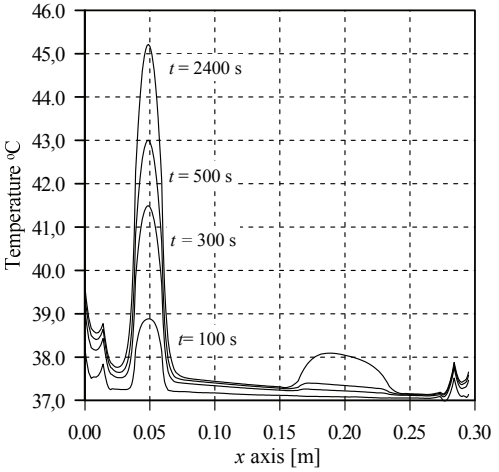

Fig.4. Temperature distribution along x axis of human thigh for different moments of time t

Temperature distribution along tumor perimeter for different time steps is presented in Fig. 6. At time $t = 2400$ [s] in all points of the tumor perimeter have temperature higher than 42°C. In Fig. 7 plot of the temperature T relative time t is

shown. On should notice that after t equal approximately 2000 [s] temperature attains steady state. This is caused mainly by big temperature capacity of the tissues.

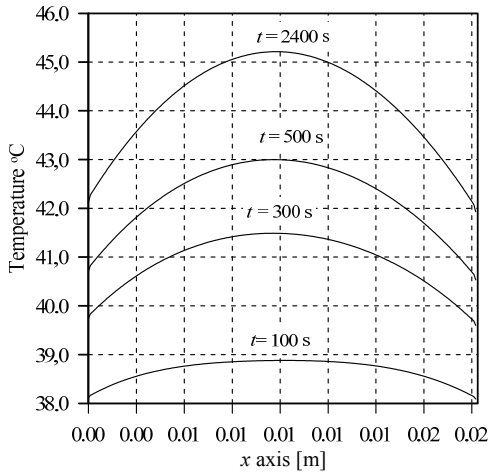

Fig.5. Temperature distribution along x axis of tumor for different moments of time t

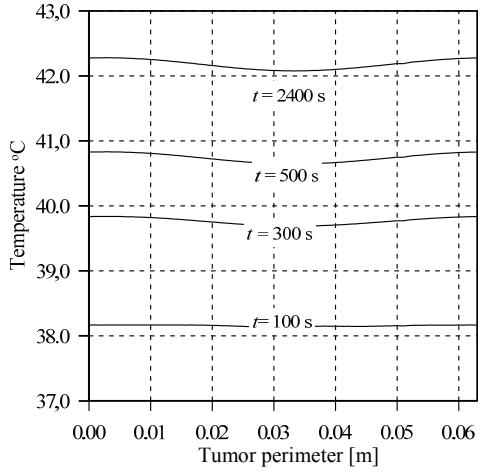

Fig.6. Temperature distribution along perimeter of the tumor for different moments of time t

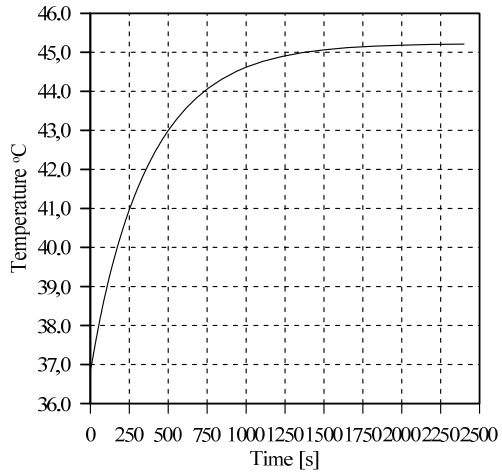

Fig.7. Time dependence of the temperature in the central point of the tumor

Summary

Theoretical studies of temperature distributions obtained with magnetic induction methods of achieving hyperthermia have been presented. The most appropriate applications of magnetic induction methods appear to be in the treatment of tumors confined to the outermost 6-7 cm of tissue in body sites with concentric coils. The numerical value of the temperature at the centre of the body surface is obtained and found to fall within the range of the values given by other numerical and experimental data reported in the literature.

It is easy to see that it is very difficult to obtain desirable temperature distribution inside the tumor and in the surrounding healthy tissues. Moreover, the temperature is very sensitive to the changes of physical parameters of the tissues and the parameters of the exciting arrangement. One needs to work out methods of temperature control that are more exact. One of the methods of temperature control in the tumor and neighbouring tissues is to place a thermometer inside the tumor. This is difficult from medical point of view and should also disturb the electromagnetic field distribution inside and outside the tumor.

REFERENCES

[1] Cassady J.R., Hamilton A., Kittelson J., Rossman K., Shetter A., Stea B.: Interstitial irradiation versus interstitial thermoradiotherapy for supratentorial malignant gliomas: a comparative survival analysis, *Int. J. Radiation Oncol. Biol. Phys.*, 30, 591 – 600, 1994.

[2] Chou C.K.: Application of electromagnetic energy in cancer treatment, *IEEE Trans. on Instrumentation and Measurements*, 37(4), 547 – 551, 1988.

[3] Clegg S.T., Das S.K., Samulski T.V.: Electromagnetic thermal therapy power optimization for multiple source applicators, *Int. J. Hyperthermia*, 15, 291 – 308, 1999.

[4] De Leeuw A.A.C., Kikuchi M., Kroeze H., Lagendijk J.J.W., Van de Kamer J.B.: Treatment planning for capacitive regional hyperthermia, *Int. J. Hyperthermia*, 19, 58 – 73, 2003.

[5] Gabriel C., Gabriely S. and Corthout E. The dielectric properties of biological tissues: I. Literature survey, *Phys. Med. Biol.*, 41, 2231 – 2249, 1996.

[6] Gas P.: Temperature Inside Tumor as Time Function in RF Hyperthermia, *Electrical Review* (*Przegląd Elektrotechniczny*), 12, 42 – 45, 2010.

[7] Gordon R.G., Horvath S.M., R.B. Roemer: A mathematical model of the human temperature regulatory system-transient cold exposure response, *IEEE Trans. Biomed. Eng.*, 23, 434 – 444, 1976.

[8] Kurgan E., Gas P.: Estimation of Temperature Distribution Inside Tissues in External RF Hyperthermia, *Electrical Review* (*Przegląd Elektrotechniczny*), 01, 100 – 102, 2010.

[9] Kuroda K., Tsuda N.: An inverse method to optimize heating conditions in RF-capacitive hyperthermia, *IEEE Trans. Biomed. Eng.*, 43, 1029-1037, 1996.

[10] Pennes, H.H., Analysis of tissue and arterial blood temperatures in resting forearm, J. Appl. Physiol., 1, 93, 1948.

[11] Roemer R.B.: Optimal power deposition in hyperthermia I. The treatment goal: the ideal temperature distribution: the role of large blood vessels, *Int. J. Hyperthermia*, 7, 317 – 341, 1991.

[12] Sullivan D.M.: Three dimensional computer simulation in deep regional hyperthermia using the finite-difference time-domain method, *IEEE Trans. Microwave Theory Tech.*, 38, 204 – 211, 1990.

***Authors**: dr hab. inż. Eugeniusz Kurgan, AGH University of Science and Technology, Department of Electrical and Power Control Engineering, al. Mickiewicza 30, 30-059 Krakow, E-mail: kurgan@agh.edu.pl, mgr inż. Piotr Gas, AGH University of Science and Technology, Department of Electrical and Power Control Engineering, al. Mickiewicza 30, 30-059 Krakow, E-mail: piotr.gas@agh.edu.pl*